



**HAL**  
open science

## Development of a gaseous proton-recoil telescope for neutron flux measurements between 0.2 and 2 MeV neutron energy

Paola Marini, Ludovic Mathieu, Mourad Aïche, Serge Czajkowski, Beatriz  
Jurado, Igor Tsekhanovich

### ► To cite this version:

Paola Marini, Ludovic Mathieu, Mourad Aïche, Serge Czajkowski, Beatriz Jurado, et al.. Development of a gaseous proton-recoil telescope for neutron flux measurements between 0.2 and 2 MeV neutron energy. *Radiat.Meas.*, 2019, 124, pp.9-12. 10.1016/j.radmeas.2019.02.013 . hal-01937452

**HAL Id: hal-01937452**

**<https://hal.science/hal-01937452>**

Submitted on 22 Oct 2021

**HAL** is a multi-disciplinary open access archive for the deposit and dissemination of scientific research documents, whether they are published or not. The documents may come from teaching and research institutions in France or abroad, or from public or private research centers.

L'archive ouverte pluridisciplinaire **HAL**, est destinée au dépôt et à la diffusion de documents scientifiques de niveau recherche, publiés ou non, émanant des établissements d'enseignement et de recherche français ou étrangers, des laboratoires publics ou privés.



Distributed under a Creative Commons Attribution - NonCommercial 4.0 International License



Contents list available at ScienceDirect

## Radiation Measurements

journal homepage: [www.elsevier.com/locate/radmeas](http://www.elsevier.com/locate/radmeas)

## Development of a gaseous proton-recoil telescope for neutron flux measurements between 0.2 and 2 MeV neutron energy

Paola Marini<sup>a</sup>, Ludovic Mathieu<sup>a</sup>, Mourad Aïche<sup>a</sup>, Serge Czajkowski<sup>a</sup>, Beatriz Jurado<sup>a</sup>, Igor Tsekhanovich<sup>a</sup><sup>a</sup>CENBG, CNRS/IN2P3-Université de Bordeaux 19, Chemin du Solarium, 33175 Gradignan, France

## HIGHLIGHTS

- ▶ A new recoil proton detector for neutron flux measurement below 1 MeV
- ▶ Low sensitivity to other particles to operate in intense electron/ $\gamma$ -rays fluxes

## ARTICLE INFO

*Article history:*

Received Click here to enter the received date

Received in revised form Revised date

Accepted Accepted date

Available on line On-line date

*Keywords:*

neutron detector

proton-recoil detector

## ABSTRACT

Absolute measurements of neutron fluence are an essential prerequisite of neutron-induced cross section measurements, neutron beam lines characterization and dosimetric investigations. The H(n,p) elastic scattering cross section is a very well known standard used to perform precise neutron flux measurements in high precision measurements. The use of this technique, with proton recoil detectors, is not straightforward below incident neutron energy of 1 MeV, due to a high background in the detected proton spectrum. Experiments have been carried out at the AIFIRA facility to investigate such background and to determine its origin and components. Based on these investigations, a gaseous proton-recoil telescope has been designed with a reduced low energy background. A first test of this detector has been carried out at the AIFIRA facility, and first results will be presented.

© 2016 Elsevier Ltd. All rights reserved

### 1. Introduction

Five out of the six concepts of new generation nuclear reactor studied in the framework of the Generation IV international forum are based on fast neutron spectra. These concepts rely on simulations based on high quality nuclear data (Aliberti et al., 2006). It is expected that the evolution of the GenIV system analysis, and the focusing on a few preferred concepts, will motivate designers to define the relevant target accuracy. Despite the experimental efforts, large discrepancies and uncertainties still exist in the actinide region (Chadwick et al., 2011). Fission cross sections are of primary importance to determine reactor behavior and incineration capabilities. As fast neutron spectra

12 are peaked between 100 keV and 2 MeV, new cross section  
13 measurements have to be performed in this energy range (NEA, 2016).

14 For neutron-induced fission cross section measurements, the  
15 accurate knowledge of the neutron flux impinging on the studied  
16 sample is mandatory. This is usually obtained measuring the fission  
17 rate of isotopes such as  $^{235}\text{U}$ ,  $^{238}\text{U}$  or  $^{237}\text{Np}$  whose reaction cross  
18 section is well known (Paradela et al., 2010, Tsinganis et al., 2014,  
19 Salvador et al., 2015, Matei et al., 2017). However, this introduces a  
20 strong correlation between independent measurements based on the  
21 same standard reactions. In addition, the accuracy of these standard  
22 reactions is limited (0.5% at best, and up to 10%). An independent and  
23 well known standard reaction is the H(n,p) elastic scattering reaction.  
24 Indeed, the detection principle is completely different from the fission

1350-4487 © Copyright Year,  
doi: 10.1016/...

1 detection, nullifying correlations between the measured cross section  
2 and the standard one. Moreover, its accuracy is about 0.2% in the MeV  
3 energy range, compared with typically few percents for the fission  
4 cross section standards mentioned above. Different concepts of proton-  
5 recoil detectors are available, depending on the type of measurements,  
6 the facility environment, the neutron energy range and the target  
7 accuracy of the measurement.

8 Plastic scintillators (Kovash et al., 2011) and proton-recoil  
9 proportional counters (Babut and Gressier, 2007, Nolte and Thomas,  
10 2011) are suited to measure low energy neutron flux, down to few 10  
11 keV. However, the scintillators require the use of time-of-flight  
12 technique to infer the neutron energy (Beyer et al., 2007), and thus can  
13 be used only in specific facility. On the other side, proportional  
14 counters provide a good accuracy of the neutron flux (2-3%), but they  
15 totally rely on simulations of the detector response.

16  
17 The use of proton-recoil telescope method is more straightforward:  
18 the neutron flux is converted into a recoil-proton flux, by mean of a  
19 hydrogenous foil called radiator. The charged protons can be easily  
20 detected, using single or multiple staged Silicon detectors (Asai et al.,  
21 2006, Donzella et al., 2010, Naitou et al., 2011, Kessedjian et al.,  
22 2012), as well as diamond detectors (Hassard et al., 1998).  
23 Nevertheless, such technique is challenging when dealing with low  
24 energy neutrons, due to background and by the energy lost in the  
25 radiator.

## 26 2. Proton-recoil detection with Si detector below 1 MeV

27 A cross section measurement was carried out by the ACEN group  
28 of the CENBG institute between 1 and 2 MeV neutron energy,  
29 produced via T(p,n) nuclear reaction at 4MV Van De Graaff facility at  
30 Bruyères-Le-Châtel, CEA, France. The proton-recoil telescope  
31 consists of a collimated 4 $\mu$ m-thick polypropylene foil (PP foil) and a  
32 collimated 50 $\mu$ m-thick Si detector placed 8 centimeters far away. The  
33 protons detected in the silicon are emitted close to 0° with respect to  
34 the incoming neutron direction, and have therefore a kinetic energy  
35 close to the incident neutron energy. They produce a peak in the  
36 proton-recoil spectrum, with a good signal-to-noise ratio. Therefore,  
37 the number of counts in the proton peak is used to determine the  
38 incident neutron flux. A detailed description of the method and of the  
39 detector itself can be found in Marini et al. (2016, 2017). Previous  
40 studies at higher energies (using multiple staged Si detector) showed  
41 that a precision of the order of 1% could be achieved in the proton  
42 peak integral (Kessedjian et al., 2012). Around 1 or 2 MeV, the  
43 accuracy is only about 3% due to a high contribution in the low energy  
44 part of the proton spectrum, as can be seen in Fig. 1. Below 1 MeV, it  
45 becomes impossible to determine the neutron flux with acceptable  
46 uncertainties. Dedicated experiments were performed on the AIFIRA  
47 facility (Sorieu et al., 2014) to investigate the origin of such  
48 background and to find solutions to reduce it. Simulations have also  
49 been carried out with the MCNP5 code, in order to improve our  
50 understanding of the observed phenomena. Results were presented in  
51 Marini et al. (2016) and are briefly summarized here.

52 The results of the MCNP simulations show that low energy  $\gamma$ -rays  
53 emitted at the neutron production source are responsible for the  
54 observed background. Indeed, they generate a large amount of  
55 electrons via Compton scattering or photoelectric effect when  
56 interacting with surrounding materials in the setup (especially the  
57 copper beam dump). Additional tests performed on the AIFIRA  
58 facility showed that this background is strongly reduced when no  
59 neutrons are produced (by using a CaF target instead of a LiF target),  
60 indicating that most of these  $\gamma$ -rays are generated by neutron radiative  
61 capture or inelastic scattering reactions, especially in the beam dump

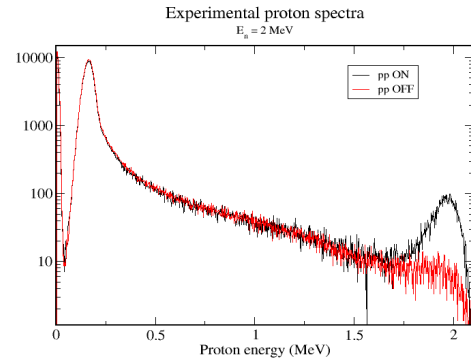


Fig. 1. Proton spectrum in the Si detector (standard and background measurements) for 2MeV incident neutron energy. The proton peak is visible on the right, as well as the intense background at low energy.

62 where the neutron flux is the highest. Electrons deposit much less  
63 energy in matter than protons due to their lower stopping power.  
64 Nevertheless, an electron of few 100 keV deposits energy in the whole  
65 thickness of the detector (here 50  $\mu$ m), whereas the ranges of 700 keV  
66 and 200 keV protons-recoil in silicon are around 10  $\mu$ m and 2  $\mu$ m  
67 respectively. In addition, simulations show that many electrons reach  
68 the Si detector with a high incident angles, further increasing the  
69 effective thickness and thus the energy deposition.

## 70 3. Development of the Gaseous Proton-Recoil Detector (GPRD)

71 To perform accurate neutron flux measurement at energies below 1  
72 MeV without relying on detector-response simulations, the ACEN  
73 group has developed a new concept of proton recoil telescope with a  
74 reduced sensitivity to  $\gamma$ -ray/electron flux. The target accuracy is 3% for  
75 neutron energies between 200 keV and 2 MeV, taking into account  
76 proton counting uncertainty, geometry uncertainty and radiator  
77 thickness uncertainty. To adapt the thickness of the detector to the  
78 proton energy, the choice was made to build a gaseous detector. The  
79 pressure can be adjusted for the total proton range in the gas to fit the  
80 detector geometry. The detector concept is similar to one of the  
81 MIMAC detector (Mayet et al., 2012), however the neutron scattering  
82 does not occur in the gas itself but in a radiator, to avoid issues  
83 specific to proportional counter detectors as presented in section 1.  
84 The detector has the capability to discriminate direct neutrons from  
85 scattered neutrons, as well as to reject contaminant events (protons  
86 emitted by other sources than PP foil, cosmic rays...), thanks to a  
87 proton track analysis. To perform accurate neutron flux measurements,  
88 the detector requires a well-defined efficiency. A scheme of the  
89 detector is presented in Fig. 2.

90 The detector is constituted by a hydrogenous radiator made of  
91 polypropylene or mylar foil and a segmented  $\Delta E$ -E ionization chamber  
92 (4x4x12cm<sup>3</sup>). The chamber is filled with CF<sub>4</sub> gas with a pressure  
93 ranging from few tens of mbar to slightly above 1 bar. The gas has  
94 been chosen free of hydrogen, to prevent additional recoil protons  
95 emission from the gas itself. Structures and collimators of the Gaseous  
96 Proton Recoil Telescope are made of Macor ceramic for the same  
97 reason. A special care was taken to build the detector with a reduced  
98 amount of material, in order to minimize the neutron scattering which  
99 seriously complicates the cross section measurement upstream the  
100 neutron flux measurement. The coincidence between the  $\Delta E$  and E  
101 sides of the ionization chamber enables a first discrimination between  
102 recoil protons and background events (such as cosmic rays or recoil  
103 proton emitted by surround H-rich materials) to be made. The track  
104 reconstruction permits the discrimination between direct and scattered

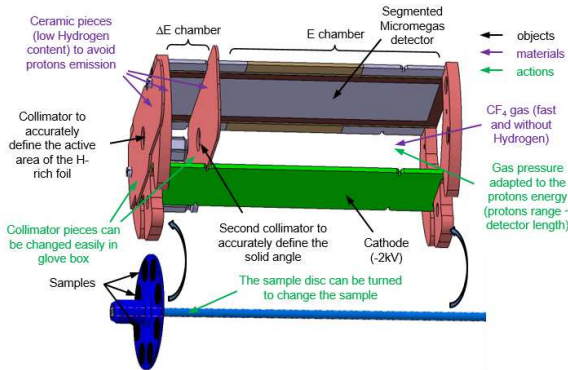


Fig. 2. Scheme of the GPRD. Objects, materials and actions are detailed. The sample disk is shown separately for clarity purpose.

1 neutrons based on the track length of the recoil proton. Indeed the  
 2 former impinge on the radiator with small angles and maximum  
 3 energy, whereas the latter lose energy in previous collisions and reach  
 4 the radiator with larger angles. Different radiators can be mounted on a  
 5 Macor rotating disk at the entrance of the detector. The rotation of the  
 6 disk step-by-step allows one to change and position the samples  
 7 without opening the chamber. An empty slot is available for  
 8 background measurements. The possibility to select the sample  
 9 thickness adapted to the neutron energy is crucial to perform  
 10 measurements on a wide energy range (from few 100 keV to few  
 11 MeV).

12 The detection plane consists in a Micromegas detector (Giomataris  
 13 et al., 1996) segmented in 64 pads as shown in the upper part of Fig. 3.  
 14 The Micromegas is able to multiply the primary electrons generated by  
 15 the recoiling proton inside the detection gas by a factor up to  $10^6$ .  
 16 Indeed, the number of primary electrons can be as low as 1000  
 17 electrons per chamber side for a 200 keV proton. The segmentation of  
 18 the detection plane enables both the reduction of the electronic noise  
 19 associated to the pad capacitance, and a raw track analysis to be  
 20 performed, in order to reject accidental coincidences with abnormal  
 21 trajectories.

22  
 23 The detector prototype was delivered at mid 2016 and a first  
 24 experiment was carried out at the AIFIRA facility to evaluate its  
 25 response and performances. Measurements were performed with  
 26 quasi-monoenergetic neutron field, with energies from 0.3 to 1 MeV,  
 27 and with a  $3\alpha$  source mounted on the sample disk. The gas pressure  
 28 was varied from 40 to 100 mbar, depending on the neutron energy, and  
 29 the applied high voltage was adapted consequently. On the first hand,  
 30 this experiment validated several expected characteristics.

31 Proton track analysis: as shown in the middle part of Fig.3, proton  
 32 tracks were detected with sufficient precision to perform abnormal  
 33 tracks rejection. In particular, proton emitted by scattered neutrons  
 34 (which have lower energies) have a shorter range and can be rejected.  
 35 Cosmic rays can also be seen, and rejected via track analysis.

36 Low sensitivity to  $e^-$  or  $\gamma$ -rays: tests carried out without the PP film  
 37 show no response of the pads. Indeed each pad is not sensitive enough  
 38 to detect the low energy deposited by electrons.

39 Low detection energy limit: neutrons with energy down to 300 keV  
 40 have been produced by the accelerator. At such low energy, as the gas  
 41 pressure could not be reduced below 40 mbar because of discharge  
 42 issues in the detection gas, the proton ranges are only of few  
 43 centimeters. As shown in the lower part of Fig.3, proton tracks are still  
 44 visible under these conditions. Improvements of the experimental  
 45 setup are necessary to lower this limit.

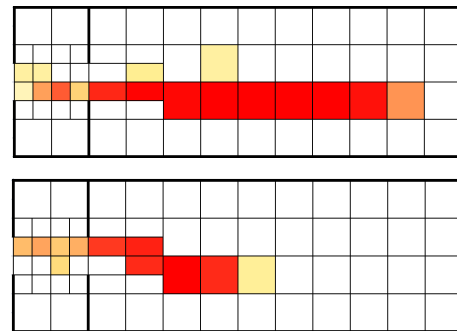
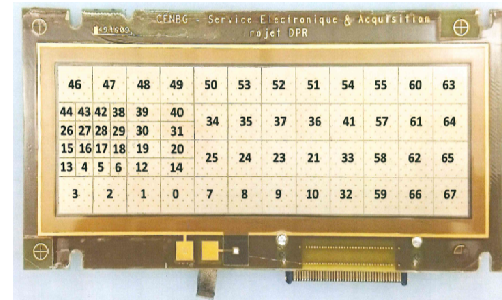


Fig. 3. (up) Picture of the segmented Micromegas detector; (middle) scheme of a proton track for a 1 MeV incident neutron energy; (down) scheme of a proton track for a 300 keV incident neutron energy

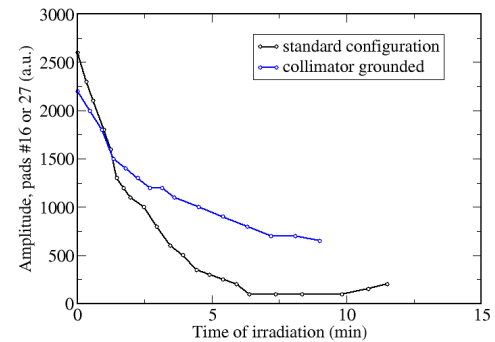


Fig. 4. Signal amplitude on pads in the  $\Delta E$  region as a function of the time of irradiation

46 These different features validate the new principle of this detector.  
 47 However, under the present experimental conditions, it was not  
 48 possible to measure the proton detection efficiency of the detector, and  
 49 in particular that every acceptable recoiling proton is actually detected.  
 50 It would have required a quantitative experiment, with the addition of  
 51 a reference fissile target.

52  
 53 On the other hand, this experiment shed light on several issues,  
 54 which prevent considering the GPRD to be operational in its current  
 55 status.

56 Static discharges: at few tens of mbar of gas pressure, the high  
 57 voltage breakdown is strongly reduced due to the Paschen law (Škoro,  
 58 2012, Marić et al., 2014). This effect was under-estimated for the  
 59 design of the detector, and discharges occurred at certain regimes  
 60 (pressure/voltage). Special care will be taken to modify the detector  
 61 design according to this constraint.

62 Non-homogeneous electric field: The detected signal amplitude of  
 63 the side pads was quite lower when compared to the central pads.

Moreover, the positioning of the collimators (see Fig. 2) also affected the signal amplitude of the neighboring pads. This is due to electric field lines not strictly perpendicular to the Micromegas and the cathode. Some of the primary electrons then drift along the field lines out of the Micromegas detection plane. To solve this issue, a field cage will be designed for the GPRD upgrade.

**Signal weakening:** Under neutron irradiation, the signal amplitude of many pads quickly decreases. As can be seen on Fig. 4, the signal is nearly lost after few minutes of irradiation. As said in section 2, a large number of low energy electrons are generated with the neutron production source. These electrons may be deposited on the surfaces of the collimators or samples disk. This induces a strong local electric field distortion, and greatly reduces the collection of primary electrons by the pads or affect their spatial distribution. Indeed, by electrically grounding the entrance collimator, the signal loss was less severe (see Fig. 4) as part of the background electrons deposited on the collimator surface are collected and removed. The addition of a field cage will solve this issue, as it will help to collect the parasitic charges and reduce the electric field lines distortion.

#### 4. Conclusion

The use of the H(n,p) standard reaction to accurately determine the neutron flux below 1 MeV without relying on detector response simulation is challenging, because the use of radiator with solid detectors is very sensitive to the high background contribution, mostly due to  $\gamma$ -rays/electrons produced in the neutron production target. To overcome this issue, a new double chamber gaseous proton-recoil telescope was designed and tested at the CENBG, with the aim of reaching an accuracy of 3% in the neutron flux determination. It has a very low sensitivity to  $\gamma$ -rays/electrons, which enables to detect recoil protons generated by incident neutron energies as low as 300 keV. Improvements have still to be made to meet the initial requirement of 200 keV neutron energy.

The  $\Delta E$ -E coincidences, coupled to a proton track analysis, enables the discrimination between direct neutrons impinging on the PP foil, scattered neutrons impinging on the PP foil, and cosmic rays or recoil proton from other H-rich surrounding materials.

However, the electric field is slightly distorted by surrounding materials, and heavily distorted by the space charge accumulation on ceramic pieces of the detector. New studies based on electrostatic simulation code to add a field cage are undertaken in order to overcome both issues. A new prototype is currently designed and will be tested in the near future.

#### Acknowledgement

This work was supported by the European Commission within the Seventh Framework Programme through Fission-2013-CHANDA (project no.605203).

#### References

G. Aliberti, G. Palmiotti, M. Salvatores, T. Kim, T. Taiwo, M. Anitescu, I. Kodeli, E. Sartori, J. Bosq, J. Tommasi, *Annals of Nuclear Energy* 33, 700 (2006)

M. Chadwick, M. Herman, P. Oblozinsky, M. Dunn, Y. Danon, A. Kahler, D. Smith, B. Pritychenko, G. Arbanas, R. Arcilla et al., *Nucl. Data Sheets* 112, 2887 (2011)

NEA, Nuclear Data High Priority Request List (2016), <http://www.nea.fr/html/dbdata/hprl>

C. Paradela and the n\_TOF collaboration, *Phys. Rev. C* 82, 034601 (2010)

A. Tsinganis and the n\_TOF collaboration, *Nucl. Data Sheets* 119, 58 (2014)

P. Salvador-Castiñeira, T. Brys, R. Eykens, F.-J. Hamsch, A. Göök, A. Moens, S. Oberstedt, G. Sibbens, D. Vanleeuw, M. Vidali, and C. Pretel, *Phys. Rev. C* 92, 044606 (2015)

C. Matei, F. Belloni, J. Heyse, A. J. M. Plompen, and D. J. Thomas, *Phys. Rev. C* 95, 024606 (2017)

M. Kovash, B. Daub, J. French, V. Henzl, K. Shoniyozov, J. Matthews, Z. Miller, H. Yang, in *Advancements in Nuclear Instrumentation Measurement Methods and their Applications (ANIMMA)*, 2nd International Conference, 1 (2011)

R. Babut, V. Gressier, *J. Instr.* 2, P01005 (2007)

R. Nolte and D.J. Thomas, *Metrologia*, 48, 274 (2011)

R. Beyer, E. Grosse, K. Heide, J. Hutsch, A. Junghans, J. Klug, D. Légrády, R. Nolte, S. Röttger, M. Sobiella et al., *Nucl. Instr. and Meth. A* 575, 449 (2007)

J. Hassard, J. Liu, R. Mongkolnavin, D. Colling, *Nucl. Instr. and Meth. A* 416, 539 (1998)

A. Donzella, M. Barbui, F. Bocci, G. Bonomi, M. Cinausero, D. Fabris, A. Fontana, E. Giroletti, M. Lunardon, S. Moretto et al., *Nucl. Instr. and Meth. A* 613, 58 (2010)

Y. Naitou, Y. Watanabe, S. Hirayama, M. Hayashi, A. Prokofiev, A. Hjalmarsson, S. Pomp, P. Andersson, R. Bevilacqua, C. Gustavsson et al., *J. Korean Phys.Soc.* 59, 1439 (2011)

G. Kessedjian, G. Barreau, M. Aïche, B. Jurado, A. Bidaud, S. Czajkowski, D. Dassié, B. Haas, L. Mathieu, L. Tassan-Got et al., *Phys. Rev. C* 85, 044613 (2012)

K. Asai, N. Naoi, T. Iguchi, K. Watanabe, J. Kawarabayashi, T. Nishitani, *J. Nuc. Sci. and Tech.* 43, 320 (2006)

P. Marini, L. Mathieu, L. Acosta, M. Aïche, S. Czajkowski, B. Jurado, I. Tsekhanovich et al., *Nucl. Instr. and Meth. A* 841, 56 (2016)

P. Marini, L. Mathieu, M. Aïche, G. Belier, S. Czajkowski, Q. Ducasse, B. Jurado, G. Kessedjian, J. Matarranz, A. Plompen, P. Salvador-Castiñeira, J. Taieb, and I. Tsekhanovich, *Phys. Rev. C* 96, 054604 (2017).

S. Sorieul, Ph. Alfaut, L. Daudin, L. Serani and Ph. Moretto, *Nucl. Instr. and Meth. B*, 332, 68 (2014)

F. Mayet, D. Santos, J. Billard, G. Bosson et al., *European Astronomical Society Publications Series*, 53, 25 (2012)

Y. Giomataris, Ph. Rebourgeard, J.P. Robert, G. Charpak, *Nucl. Instr. and Meth. A*, 376, 29 (1996)

N. Škoro, *J. Phys. Conf. Series* 399, 012017 (2012)

D. Marić, M. Savić, J. Sivoš, N. Škoro, M. Radmilović-Radjenović, G. Malović, Z. L. Petrović, *Eur. Phys. J. D* (2014)